

LETTERS

The *ERECTA* gene regulates plant transpiration efficiency in *Arabidopsis*

Josette Masle¹, Scott R. Gilmore¹ & Graham D. Farquhar¹

Assimilation of carbon by plants incurs water costs. In the many parts of the world where water is in short supply, plant transpiration efficiency, the ratio of carbon fixation to water loss, is critical to plant survival, crop yield and vegetation dynamics¹. When challenged by variations in their environment, plants often seem to coordinate photosynthesis and transpiration², but significant genetic variation in transpiration efficiency has been identified both between and within species^{3,4}. This has allowed plant breeders to develop effective selection programmes for the improved transpiration efficiency of crops⁵, after it was demonstrated that carbon isotopic discrimination, Δ , of plant matter was a reliable and sensitive marker negatively related to variation in transpiration efficiency^{3,4,6}. However, little is known of the genetic controls of transpiration efficiency. Here we report the isolation of a gene that regulates transpiration efficiency, *ERECTA*. We show that *ERECTA*, a putative leucine-rich repeat receptor-like kinase (LRR-RLK)^{7,8} known for its effects on inflorescence development^{7,9}, is a major contributor to a locus for Δ on *Arabidopsis* chromosome 2. Mechanisms include, but are not limited to, effects on stomatal density, epidermal cell expansion, mesophyll cell proliferation and cell–cell contact.

We have previously demonstrated considerable natural variation in leaf carbon isotopic discrimination (Δ) among *Arabidopsis* accessions, and established that this variation fits the predicted pattern of a linear relationship with the ratio p_i/p_a of intercellular to ambient CO₂ partial pressure within the leaf¹⁰, and hence with transpiration efficiency⁶. We therefore used Δ as a tool to assess the phenotype of a population of recombinant, inbred lines derived from a cross between Col-4 and Ler¹¹ ecotypes for variation in transpiration efficiency, with the aim of identifying genetic loci associated with this trait. Over the last 15 yr putative quantitative trait loci (QTL) for transpiration efficiency or carbon isotope discrimination have been identified in various species^{12,13}; however, none of the contributing genes has been identified. Ribulose 1,5-bisphosphate carboxylase-oxygenase (Rubisco) activase has been suggested as a candidate gene controlling transpiration efficiency in tomato¹⁴, but these results have not been confirmed. Our analysis revealed a significant QTL for rosette Δ on chromosome 2 (Fig. 1a), which, depending on growth conditions, explained 21–64% of the total phenotypic variation in Δ (see Supplementary Table 1).

That QTL, hereafter referred to as transpiration efficiency 1 (TE1), covered a small region of about 37 genes centred on the 'er' marker (the *ERECTA* gene itself, At2g26330) at map position 50.64 cM. Furthermore, the distributions of Δ values for the subpopulations of recombinant lines carrying the *er1* and *ERECTA* alleles were always offset, with the mean values systematically lower for the latter population (Supplementary Table 1), indicative of significantly greater transpiration efficiency. This led us to test directly the effect of the *ERECTA* gene itself on Δ and transpiration efficiency.

As a first step, we compared Δ for three *erecta* mutants (*Coler2*,

Coler105 and *Ler*) to that of near-isogenic background lines homozygous for the *ERECTA* allele (*Col-0*, *Col-0/Col-1* and *N163/N3177*, respectively). In each case, the *erecta* line displayed a higher Δ than the line homozygous for the *ERECTA* allele (Fig. 1b). This was especially so for *Coler105*, which on average differed from *Col-0* by 1.1 per mil (that is, the ¹²C/¹³C ratio of the genotypes differed by

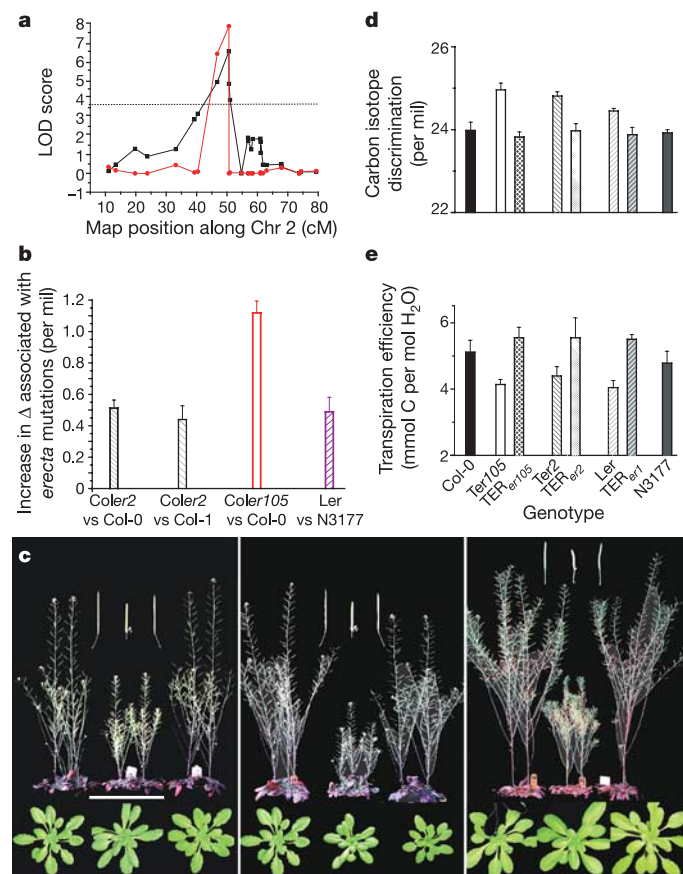


Figure 1 | *ERECTA*, a transpiration efficiency gene. **a**, A QTL for Δ on *Arabidopsis* chromosome 2 (48.96–51.02 cM). Simple (black symbols) and composite (red symbols) interval mapping. The dotted line indicates 1% LOD significance level. **b**, *Erecta* mutations cause increased Δ . Error bars denote s.e.m. **c**, Conversion of morphological phenotype of *Coler2*, *Coler105* and *Ler* (left, middle and right panels, respectively) by complementation with *ERECTA*. Left to right in each set of photographs: ER ecotype; *erecta* mutant; complemented *TER_{er1}* line. Scale bar, 75 mm (rosettes), 180 mm (mature plants), 30 mm (pods). **d**, **e**, Mutant complementation restores wild-type Δ and transpiration efficiency values (data are mean \pm s.e.m.).

¹Environmental Biology Group, Research School of Biological Sciences, The Australian National University, Canberra, ACT 2601, Australia.

1.1×10^{-3} times the $^{12}\text{C}/^{13}\text{C}$ ratio of the source CO_2), implying an approximately 20% decrease in transpiration efficiency under our growth conditions. The *Coler105* mutant carries a null allele and is characterized by an absence of *ERECTA* transcripts^{7,15}. The *Coler2* and *Ler* mutants, which both carry an I to K amino acid change in the protein kinase domain⁸, showed an increase of 0.4–0.5 per mil in Δ compared to the isogenic ER (*ERECTA*) line.

To confirm the role of *ERECTA* in these differences, we transformed the *Coler2* and *Coler105* mutants with a pKUT196 construct carrying the Col-0 *ERECTA* gene (see Methods). All transgenic plants showed a typical *ERECTA* phenotype, indistinguishable from that of Col-0 or Col-1 (Fig. 1c). The abundance of *ERECTA* transcripts in the transgenic plants relative to that in Col-0 varied over roughly an order of magnitude depending on line (Supplementary Fig. 1). Ten independent T3 Columbia transgenic lines (denoted as *TER_{er2}* and *TER_{er105}* below) homozygous for the *ERECTA* transgene were selected for evaluation of Δ . All showed significantly reduced Δ values compared with the parental *Ter2* and *Ter105* mutant lines, resulting in values similar (Fig. 1d) or even lower (Supplementary Table 2) than those measured in Col ER ecotypes. Leaf transpiration efficiency was directly measured on the same plants by gas exchange techniques and, consistent with theory⁶, showed variations opposite to those in Δ (Fig. 1e). These results were further confirmed by the analysis of a transgenic Landsberg ER line (*TER_{er1}*), a transformant of *Ler* also complemented with the pKUT196 construct¹⁶ and showing typical *ERECTA* phenotype (Fig. 1c, right panel). The *TER_{er1}* line also displayed much lower Δ than *Ler* (Fig. 1d) and an improved transpiration efficiency (Fig. 1e), similar to or better than that measured in near-isogenic *ERECTA* lines N3177 or N163. These data demonstrate that *ERECTA* is directly involved in the control of leaf Δ and transpiration efficiency.

Leaf transpiration efficiency describes the ratio of photosynthesis to transpiration rates. Genetic variation in transpiration efficiency could arise from variation in either of these components. To determine the mode of action of *ERECTA* on transpiration efficiency and the underlying leaf properties, we first examined its effects on stomatal conductance, a driver of transpiration rate. This revealed that *Coler2*, *Coler105* and *Ler* mutants are all characterized by a much higher leaf stomatal conductance than the parental ER ecotype. Complementing these mutants with *ERECTA* markedly lowered stomatal conductance, restoring values similar to those observed in ER ecotypes (Fig. 2a). To examine whether *ERECTA* also modulates biochemical limitations to photosynthesis, we examined the response of the CO_2 assimilation rate to intercellular partial pressure of CO_2 (p_i) under saturating light, a diagnostic of variation in photosynthetic capacity. Data for all individual leaves could be well described by a biochemical model¹⁷ in which, under low ambient CO_2 concentrations, CO_2 assimilation is limited by the ribulose-1,5-bisphosphate (RuBP)-saturated rate of Rubisco carboxylation, whereas under high concentrations, CO_2 assimilation is determined by the rate of RuBP regeneration (see example in Fig. 2b). Using this model, we derived estimates of maximum Rubisco carboxylation rate (V_{cmax} , related to the initial slope in Fig. 2b) and electron transport rate (J_{max} , related to the plateau in Fig. 2b). The *er2* mutation and to a lesser extent the *er105* mutation in the Columbia ecotype both depressed these rates, whereas the *er1* mutation in the Landsberg ecotype had no significant effect. These data on V_{cmax} and J_{max} demonstrate a role for the *ERECTA* gene in controlling leaf photosynthetic capacity and balancing biochemical and stomatal limitations on photosynthesis. They also indicate that this function of *ERECTA* is dependent on genetic background and is modulated by other genetic polymorphisms between the two ecotypes.

ERECTA has recently been implicated in the control of tissue patterning in stems and pedicels^{18,19}. This led us to hypothesize that its effects on leaf gas exchange properties may partially reflect a role in the development of vegetative organs, leaves in particular, thereby impacting on stomatal conductance and CO_2 carboxylation capacity

within the lamina. To test this hypothesis we examined the anatomy of the mature leaves used for gas exchange measurements, or of leaves of similar age. These observations revealed a greatly increased stomatal density in all three *erecta* mutants analysed (Fig. 3a), largely explaining their increased stomatal conductance (Fig. 3b). These leaves also displayed much smaller epidermal cells than leaves of ER lines (Fig. 3c), so that there was no significant change in stomatal index (Fig. 3d; see Methods for definition). Thus, *ERECTA* seems to modulate stomatal density mostly through a role in epidermal pavement cell expansion rather than in stomatal development and patterning *per se*²⁰.

There was no systematic difference in blade thickness between lines, but in *Ter2* and *Ter105* the anatomy of the mesophyll tissue was distinctly different compared with that in complemented *ER* lines or Col-0/Col-1 ecotypes, with fewer, looser packed mesophyll cells, especially in the spongy mesophyll (Fig. 3e). The measured reduction

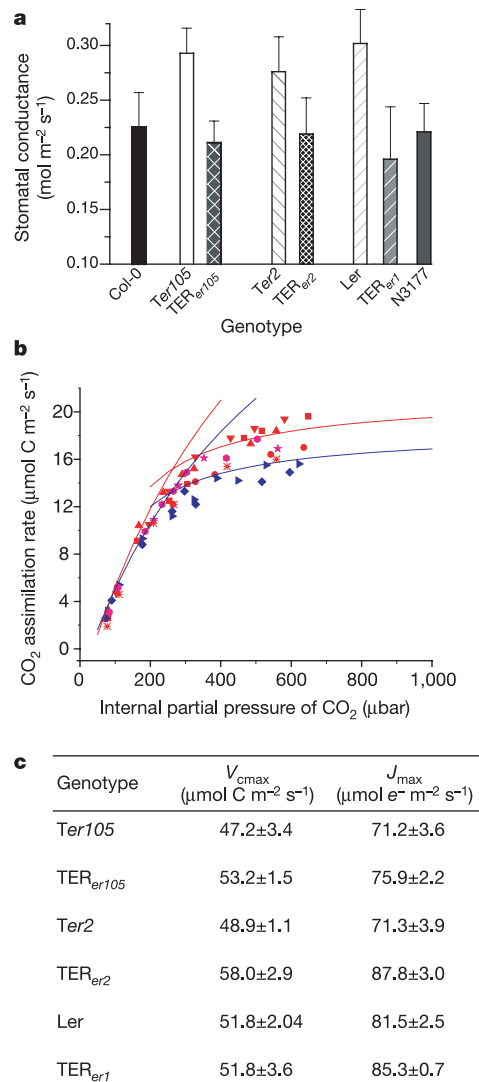


Figure 2 | *ERECTA* regulates leaf gas exchange. **a**, Stomatal conductance to diffusion of water vapour calculated from gas exchange measurements on mature leaves (same plants as in Fig. 1d, e; error bars indicate s.e.m.). **b**, Relationships between CO_2 assimilation rate, measured under saturating light, and internal partial pressure of CO_2 in the substomatal cavity for *Coler2* (blue points) and complemented *TER_{er2}* plants (red points). Two-branch curves: theoretical relationships¹⁷. **c**, Electron transport capacity (J_{max}) and maximum Rubisco carboxylation rates (V_{cmax}) derived from the theoretical relationships such as those in **b**, for three *erecta* mutants and the complemented transgenic *ERECTA* lines.

of photosynthetic capacity (Fig. 2b, c) suggests that the reduction in the amount of photosynthetic machinery per unit leaf area more than offsets the benefits of greater porosity within the leaf²¹. Such anatomical features were hardly detectable and less systematic in the Ler mutant compared to its near-isogenic N163/N3177 or transgenic *TER_{er1}* lines, also consistent with the absence of a significant difference in V_{cmax} or J_{max} between those lines (Fig. 2c).

These data provide direct evidence that *ERECTA* is involved in leaf organogenesis and modulates cell expansion, cell division and cell–cell contact within leaves in a manner dependent on genetic background. Through these effects *ERECTA* modifies leaf diffusive properties and mesophyll capacity for photosynthesis, and thereby the trade-off between water loss through stomata and assimilated CO_2 . A role of *ERECTA* in cell–cell and tissue–tissue signalling within leaves is consistent with its putative molecular identity as a LRR-RLK, and its broad expression in the shoot apical meristem and leaf primordia²². It has also recently been shown that *ERECTA* participates in the establishment of abaxial–adaxial polarity in leaf primordia²³ and in the control of cell proliferation and differentiation in the inflorescence^{15,18}. Nevertheless, it is significant that even in the Landsberg background of Ler, where the effects of the mutation on mesophyll anatomy were small, the coordinated effect of the ER complementation on Δ , p_i/p_a and transpiration efficiency was still large, similar to that in the Columbia background (for example,

$\Delta(\text{Ler}) - \Delta(\text{TER}_{er1}) = 0.83$ per mil, corresponding to a 16% difference in transpiration efficiency). It is therefore tempting to conclude that *ERECTA* does not affect transpiration efficiency solely through developmental mechanisms, but possibly through a separate pathway.

Plant transpiration efficiency, leaf development and gas exchange properties are strongly modulated by environmental factors, in particular those influencing plant water status⁴. That *ERECTA* improves transpiration efficiency under well-watered conditions does not necessarily imply that this should still be the case in dry environments where, from an ecological perspective, such a function would matter most. To test this proposition we challenged *erecta* mutants and near-isogenic ER lines with soil drought or low air humidity at constant leaf temperature. The *erecta* mutations conferred reduced leaf transpiration efficiency across the whole range of environments, and gene complementation led to restoration of higher transpiration efficiency, to levels similar to ER ecotypes (Fig. 4a). Similar observations held for long-term, whole-plant water use efficiency (Fig. 4b) measured over a drought period, which reduced plant growth by 20–30% depending on line.

We have identified a new function for the *ERECTA* gene in the control of transpiration efficiency. *ERECTA* is, to our knowledge, the first gene to be shown to act on the coordination between transpiration and photosynthesis, and therefore to be identified as

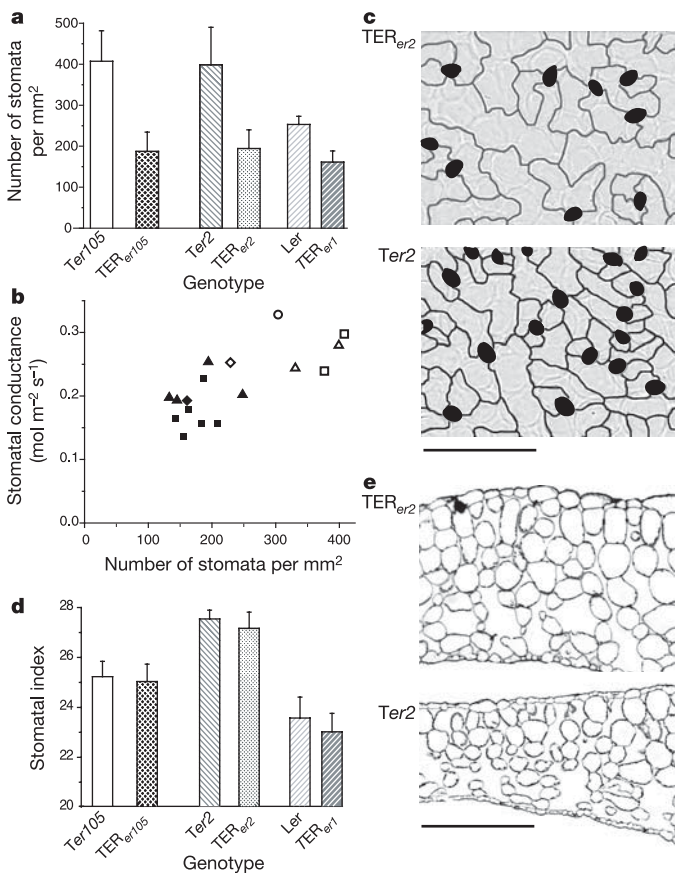


Figure 3 | Leaf anatomical features contributing to the effects of *ERECTA* on transpiration efficiency. **a**, Stomatal densities (means ± s.e.m.; adaxial epidermis). **b**, Relationship between stomatal conductance and stomatal density. Open symbols, *Ter2* (squares), *Ter105* (triangles) and *Ler* (diamonds); filled symbols, complemented lines. **c**, Coordinated effects of *ERECTA* on epidermal cell size and stomatal densities (data for adaxial epidermis, same pair of lines as for **a** with contours of cells outlined to facilitate comparison; scale bar, 155 μm). **d**, Stomatal index was unchanged. **e**, Cross-sections of leaves showing reduced mesophyll development and increased intercellular spaces in *erecta* leaves. Scale bar, 150 μm .

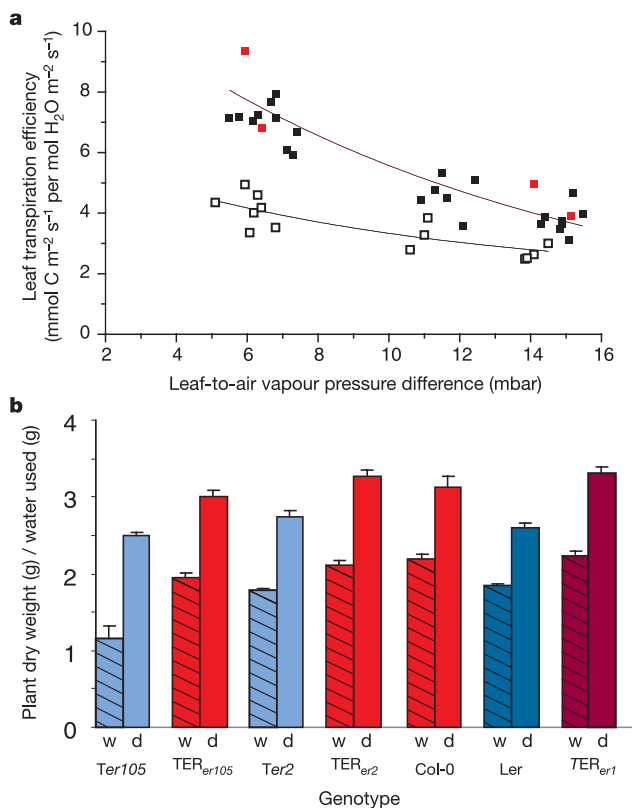


Figure 4 | *ERECTA* improved transpiration efficiency under both well-watered and drought conditions. **a**, Response of instantaneous leaf transpiration efficiency to leaf-to-air vapour pressure difference for *Ter105* (open squares) and *TER_{er105}* (black squares) or *Col-0* (red squares). Vapour pressure difference was varied by changing the humidity of air entering the chamber, keeping leaf temperature constant. Lines were fitted by nonlinear regression; ER plants had greater transpiration efficiency along the whole vapour pressure difference range. **b**, Whole-plant water use efficiency (days 16–30) for well-watered plants or those under drought conditions (labelled w or d, respectively on the x axis). Blue shades indicate *erecta* mutants (*Ter105*, *Ter2* and *Ler*); red shades indicate complemented TER lines and *Col-0*. Error bars indicate s.e.m.

a transpiration efficiency gene, as opposed to simply a stomatal or photosynthesis gene. We show that *ERECTA* can modify transpiration efficiency by acting on epidermal and mesophyll development, stomatal density and the porosity of leaves. Furthermore, even in backgrounds where changes in the mesophyll are small, the coordinated change in transpiration efficiency, as revealed by Δ or p_i/p_a , is still large. We have identified *ERECTA* homologues in diverse species (Supplementary Fig. 2 and our own unpublished observations). Phylogenetic analysis of these sequences shows that *ERECTA* has evolved during or before early angiosperm evolution. It is therefore not totally surprising that it should have a function in a trait like transpiration efficiency, which is of major importance for plant fitness and competitive ability under the selective pressure of one of the most variable and often limiting soil resources. The large magnitude of changes associated with complementation of null mutants suggests that *ERECTA* may be acting as a master gene. In several transgenic ER lines, Δ was decreased considerably below wild-type values, without detectable growth penalty, indicating the potential for manipulating *ERECTA* as a path towards improved crop performance. The ability to manipulate *ERECTA* in genetically and ecologically diverse species enhances prospects of deciphering its mode of action on the coordination between stomatal conductance and mesophyll capacity for photosynthesis at the molecular and cellular level, and of identifying the pathways involved. It will also assist in designing strategies for improved transpiration efficiency under dry conditions on the one hand, and removal of stomatal limitations and increase of yield potential in well-watered conditions on the other. Our data demonstrate that Δ constitutes a sensitive and integrative phenotypic marker of the effects of *ERECTA* on transpiration efficiency and underlying leaf gas exchange properties, opening great promise for evaluating the usefulness of this gene for breeding crop species⁵.

METHODS

Plant material and growth conditions. Recombinant inbred lines were grown in controlled glasshouses or chambers under several combinations of irradiance, light spectrum, photoperiod, atmospheric humidity and temperature (see Supplementary Table 1). *Erecta* mutants, complemented transgenic lines (denoted as TER_{er1}, TER_{er2} and TER_{er105}) and near-isogenic Columbia and Landsberg ecotypes were grown in a controlled chamber (10h photoperiod, 21 °C day/night, 400 $\mu\text{mol quanta m}^{-2} \text{s}^{-1}$ after acclimation at 100 $\mu\text{mol quanta m}^{-2} \text{s}^{-1}$). Water was continuously supplied to roots by capillarity, keeping plants well watered except for the 'drought' treatment (labelled 'd' in Fig. 4b), where from day 16 half of the plants were fed 60% only of the water used by control, well-watered plants of similar size. That regime led to a progressive water stress, causing an approximately 25% reduction in plant mass over 2.5 weeks compared to well-watered plants.

We generated the transgenic Columbia lines TER_{er2} and TER_{er105} by complementation of *erecta* mutants *er2* and *er105*, respectively, with pKUT196, a plasmid containing the entire *ERECTA* locus from Columbia¹⁵ (see Supplementary Information for details of plant transformation and confirmation of *ERECTA* expression by quantitative PCR). The TER_{er1} Landsberg line (*Ler* mutant also complemented with the pKUT196 plasmid) was a gift from K. Torii. All other seeds were obtained from Nottingham Arabidopsis Stock Centre (stock N1899 (Recombinant Inbred Lines), N933 (Col-4), NW20 (*Ler*), N1093 (Col-0), N3176 (Col-1) and N163/N3177).

Carbon isotope discrimination. Analysis of carbon isotope composition was performed as described (see Supplementary Methods) on 4–5-week-old rosettes (50–70% of final size, vegetative stage or first flower buds just visible) from 4–6 plants per line. For the comparison of *erecta* mutants with near-isogenic *ERECTA* lines, an additional analysis was done at the time of gas exchange measurements and microscopy analysis, when 10–50% of flowers to be produced were opened. Carbon isotope discrimination was calculated as described (see Supplementary Methods).

QTL analysis of carbon isotopic discrimination. QTL analysis was done by simple and composite interval mapping^{24,25} using QTL Cartographer²⁶ run as described for cofactor selection²⁷. Walking speed and window size within model 6 (CIM) were left at default settings. Significant LOD (log likelihood ratios) threshold values were determined by running 1,000 permutations using the CIM model.

Physiological analyses. Physiological analyses were done on ten independent T3 transformants homozygous for the *ERECTA* transgene (lines denoted TER_{er1}, TER_{er2} and TER_{er105}, where the subscript denotes the *erecta* allele carried by the original mutant). These lines were compared to *erecta* mutants (*Ler* or negative T3 transformants *Ter2* and *Ter105*) as well as to the original mutants and to near-isogenic ER ecotypes Col-0 and Col-1 or N3177 and N163.

Rates of CO₂ assimilation (A) and transpiration (E) were measured in an open gas-exchange system, set up with a whole-leaf clamp-on chamber. Measurements were made on a young, fully expanded rosette leaf (on 4–8 plants per line and water supply treatment) at an irradiance of 500 $\mu\text{mol quanta m}^{-2} \text{s}^{-1}$, and leaf temperature of 22 °C. The first measurement was made at growth p_a (350 μbar) and a leaf-to-air vapour difference of 8–10 mbar; then either p_a or leaf-to-air vapour difference was varied to examine their effects on the rate of CO₂ assimilation. Calculations of gas exchange parameters were as described²⁸. Instantaneous leaf transpiration efficiency was calculated as the ratio A/E.

From gas exchange measurements of CO₂ assimilation and p_i , *in vivo* estimates of the maximum rate of Rubisco carboxylation (V_{cmax}) and electron transport capacity (J_{max}) were obtained²⁹, assuming no limitation to the conductance for transfer of CO₂ between the substomatal cavities and the sites of carboxylation.

In the drought experiment, whole-plant water use efficiency was calculated from gravimetric measurements of increase in plant dry weight (day 16 to day 30) and water loss, providing an integrative measure over time and over the whole plant that also takes into account respiratory losses.

Leaf anatomy. Mature rosette leaves (leaves used for gas exchange or of similar age: three leaves per rosette and 4–6 replicated rosettes per line) were cleared and mounted on a light microscope fitted with a video camera for measurements of epidermal cell size (MTV program, Datacrunch), identification of stomatal complexes on both adaxial and abaxial epidermis, and determination of stomatal index ($100 \times \text{stomatal density} / (\text{stomatal density} + \text{epidermal cell density})$). These observations were performed on three small areas ($36\text{--}38 \times 10^3 \mu\text{m}^2$) selected on each side of the blade, symmetrical about the main vein. Before clearing, a small blade section was cut out mid-way along the blade, and fixed in 2.5% (v/v) glutaraldehyde, post-fixed in 1% (v/v) osmium tetroxide in 25 mM phosphate buffer, pH 7.0, slowly dehydrated in ethanol and embedded in Spurr's resin. Cross-sections were stained with toluidine blue and mounted on a light microscope fitted with a CCD camera for observation of mesophyll anatomy.

Data analysis. Statistical significance of results was tested by analysis of variance (ANOVA). Curves in Fig. 3 were fitted by nonlinear regression using ORIGIN7 (Microcal Software Inc.) statistical functions.

Received 13 January; accepted 19 May 2005.

Published online 10 July 2005.

- Boyer, J. S. Plant productivity and environment. *Science* **218**, 443–448 (1982).
- Wong, S. C., Cowan, I. R. & Farquhar, G. D. Stomatal conductance correlates with photosynthetic capacity. *Nature* **282**, 424–426 (1979).
- Farquhar, G. D., Ball, M. C., von Caemmerer, S. & Roksandic, Z. Effect of salinity and humidity on $\delta^{13}\text{C}$ values of halophytes—evidence of diffusional isotope fractionation determined by the ratio of intercellular/atmospheric partial pressure of CO₂ under different environmental conditions. *Oecologia* **52**, 121–124 (1982).
- Farquhar, G. D. & Richards, R. A. Isotopic composition of plant carbon correlates with water-use efficiency of wheat genotypes. *Aust. J. Plant Physiol.* **11**, 539–552 (1984).
- Rebetzke, G. J., Condon, A. G., Richards, R. A. & Farquhar, G. D. Selection for reduced carbon isotope discrimination increases aerial biomass and grain yield of rain fed bread wheat. *Crop Sci.* **42**, 739–745 (2002).
- Farquhar, G. D., O'Leary, M. H. & Berry, J. A. On the relationship between carbon isotopic discrimination and intercellular carbon dioxide concentration in leaves. *Aust. J. Plant Physiol.* **9**, 121–137 (1982).
- Torii, K. U. et al. The *Arabidopsis ERECTA* gene encodes a putative receptor protein kinase with extracellular leucine-rich repeats. *Plant Cell* **8**, 735–746 (1996).
- Lease, K. A., Lau, N. Y., Schuster, R. A., Torii, K. U. & Walker, J. C. Receptor serine/threonine protein kinases in signalling: analysis of the *ERECTA* receptor-like kinase of *Arabidopsis thaliana*. *New Phytol.* **151**, 133–143 (2001).
- Bowman, J. in *Arabidopsis: An atlas of morphology and development* (ed. Bowman, J.) (Springer, New York, 1994).
- Masle, J., Shin, J. S. & Farquhar, G. D. in *Perspectives of Plant Carbon and Water Relations from Stable Isotopes* (eds Ehleringer, J., Hall, A. E. & Farquhar, G. D.) 371–386 (Academic, New York, 1993).
- Lister, C. & Dean, C. Recombinant inbred lines for mapping RFLP and phenotypic markers in *Arabidopsis thaliana*. *Plant J.* **4**, 745–750 (1993).
- Martin, B., Nienhuis, J., King, G. & Schaefer, A. Restriction fragment length

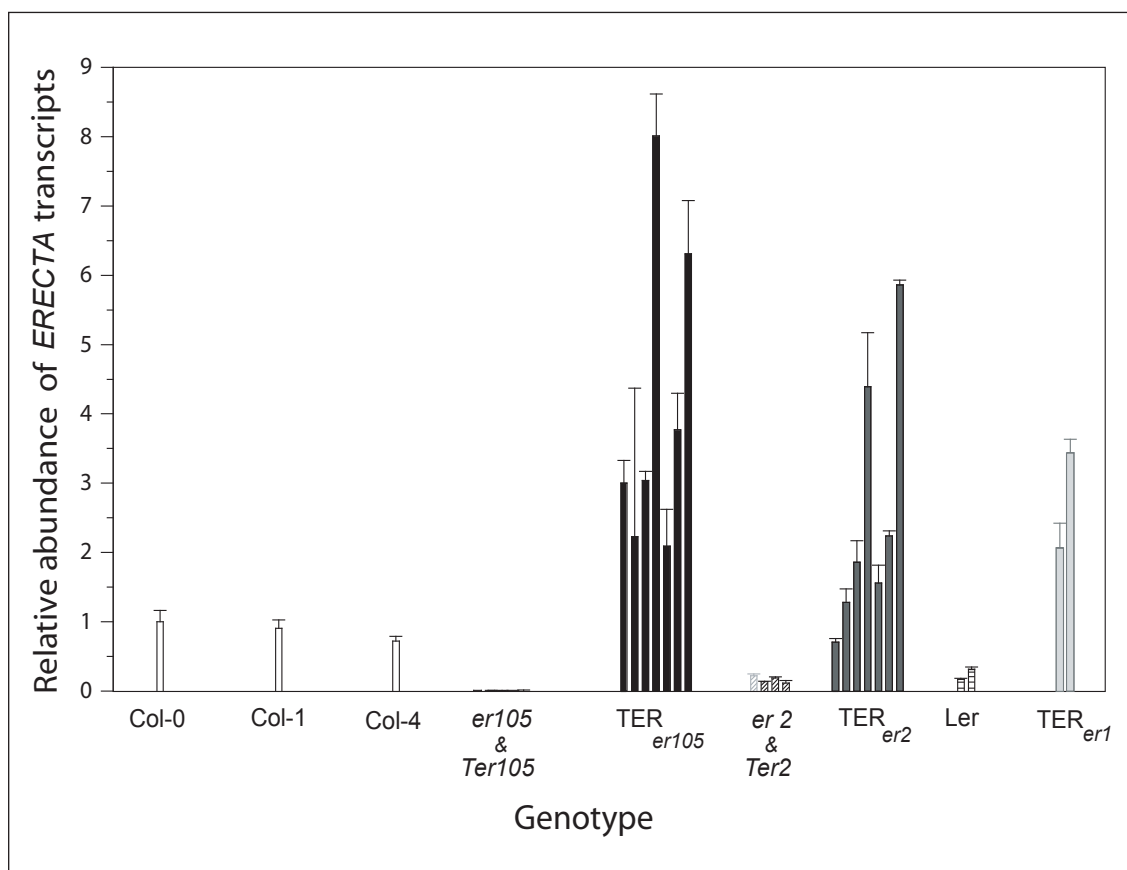
- polymorphisms associated with water-use efficiency in tomato. *Science* **243**, 1725–1728 (1989).
13. Thumma, B. R. *et al.* Identification of causal relationships among traits related to drought resistance in *Stylosanthes scabra* using QTL analysis. *J. Exp. Bot.* **52**, 203–214 (2001).
 14. Zhu, Y., Kuanhung, R. L., Huang, Y., Tauer, C. G. & Martin, B. A cDNA from tomato (*Lycopersicon pennellii*) encoding ribulose-1,5-bisphosphate carboxylase/oxygenase activase (accession No. AF037361) (PGR98–053). *Plant Gene Register* **116**, 1603 (1998).
 15. Shpak, E. D., Lakeman, M. B. & Torii, K. U. Dominant-negative receptor uncovers redundancy in the *Arabidopsis* *ERECTA* leucine-rich repeat receptor-like kinase signalling pathway that regulates organ shape. *Plant Cell* **15**, 1095–1110 (2003).
 16. Godiard, L. *et al.* *ERECTA*, an LRR receptor-like kinase protein controlling development pleiotropically affects resistance to bacterial wilt. *Plant J.* **36**, 353–365 (2003).
 17. Farquhar, G. D., von Caemmerer, S. & Berry, J. A. A biochemical model of photosynthetic CO₂ assimilation in leaves of C₃ species. *Planta* **149**, 78–90 (1980).
 18. Douglas, S. J., Chuck, G., Dengler, R. E., Pelecanda, L. & Riggs, C. D. *KNAT1* and *ERECTA* regulate inflorescence architecture in *Arabidopsis*. *Plant Cell* **14**, 547–558 (2002).
 19. Shpak, E. D., Berthiaume, C. T., Hill, E. J. & Torii, K. U. Synergistic interaction of three *ERECTA*-family receptor-like kinases controls *Arabidopsis* organ growth and flower development by promoting cell proliferation. *Development* **131**, 1491–1501 (2004).
 20. Nadeau, J. A. & Sachs, F. D. in *The Arabidopsis Book* (eds Somerville, C. & Meyerowitz, E.) 1–28 (<http://www.aspb.org/publications/arabidopsis/>) (American Society of Plant Biologists, Rockville, Maryland, 2002).
 21. Farquhar, G. D. & Raschke, K. On the resistance to transpiration of the sites of evaporation within the leaf. *Plant Physiol.* **61**, 1000–1005 (1978).
 22. Yokoyama, R., Takahashi, T., Kato, A., Torii, K. U. & Komeda, Y. The *Arabidopsis* *ERECTA* gene is expressed in the shoot apical meristem and organ primordia. *Plant J.* **15**, 301–310 (1998).
 23. Xu, L. *et al.* Novel *as1* and *as2* defects in leaf adaxial-abaxial polarity reveal the requirement for *ASYMMETRIC LEAVES1* and *2* and *ERECTA* functions in specifying leaf adaxial identity. *Development* **130**, 4097–4107 (2003).
 24. Lander, E. S. & Botstein, D. Mapping Mendelian factors underlying quantitative traits using RFLP linkage maps. *Genetics* **121**, 185–199 (1989).
 25. Zeng, Z.-B. Precision mapping of Quantitative Trait Loci. *Genetics* **136**, 1457–1468 (1994).
 26. Basten, C., Weir, B. & Zeng, Z.-B. *QTL Cartographer* (North Carolina State Univ., Raleigh, North Carolina, 2000).
 27. Loudet, O., Chailou, S., Camilleri, C., Bouchez, D. & Daniel-Vedele, F. Bay-0 x Shahdara recombinant inbred line population: a powerful tool for the genetic dissection of complex traits in *Arabidopsis*. *Theor. Appl. Genet.* **104**, 1173–1184 (2002).
 28. von Caemmerer, S. & Farquhar, G. D. Some relationships between the biochemistry of photosynthesis and the gas exchange of leaves. *Planta* **153**, 376–387 (1981).
 29. Masle, J., Hudson, G. S. & Badger, M. R. Effects of ambient CO₂ concentration on growth and nitrogen use in tobacco (*Nicotiana tabacum*) plants transformed with an antisense gene to the small subunit of Ribulose-1,5-bisphosphate carboxylase/oxygenase. *Plant Physiol.* **103**, 1075–1088 (1993).

Supplementary Information is linked to the online version of the paper at www.nature.com/nature.

Acknowledgements We thank K. Torii for the pKUT196 plasmid, T. Baskin for *Coler105* seeds, and S. May, C. Somerville, S. C. Wong, R. Jost and O. Berkowitz for helpful discussions, encouragement and/or comments on the manuscript.

Author Information Reprints and permissions information is available at npg.nature.com/reprintsandpermissions. The authors declare no competing financial interests. Correspondence and requests for materials should be addressed to J.M. (josette.masle@anu.edu.au).

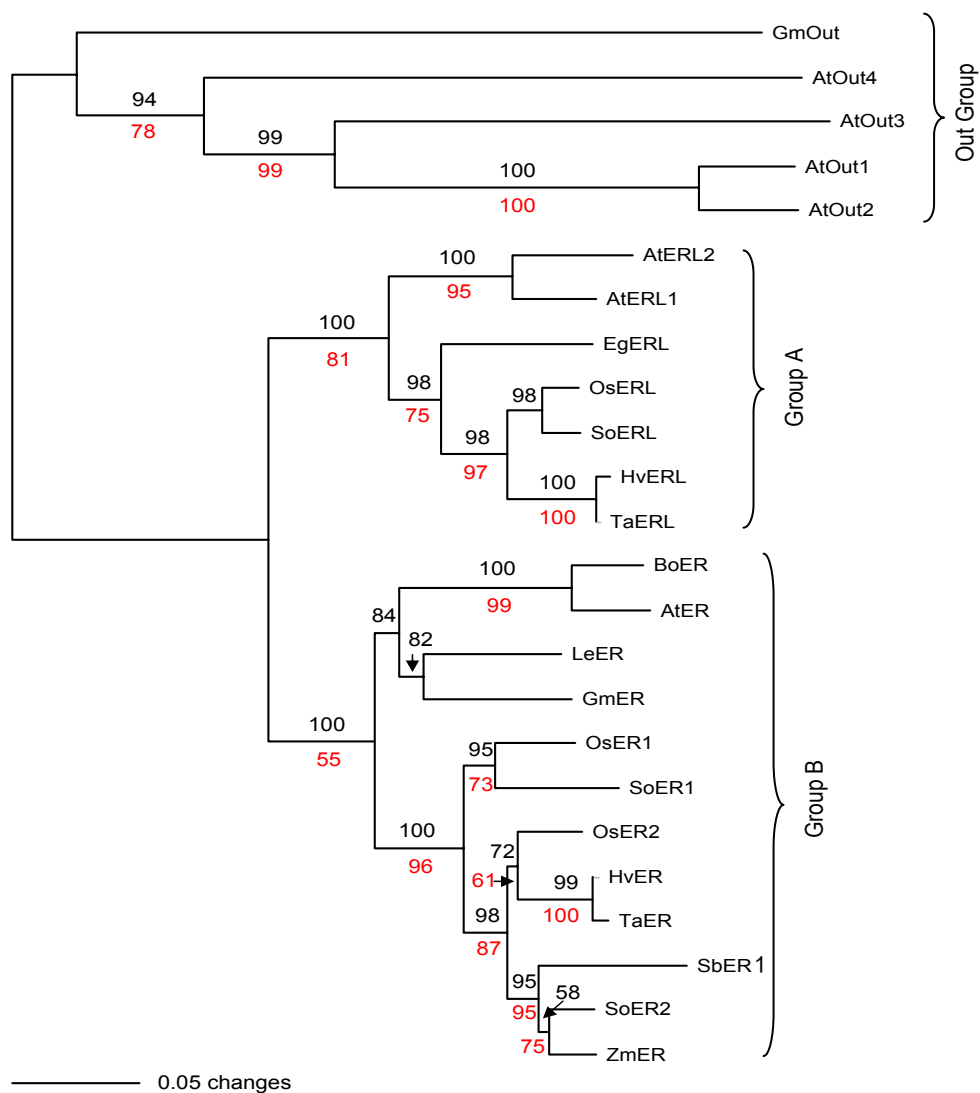
Supplementary Figure 1



Relative abundance of *ERECTA* (At2g26330) transcripts normalised to transcripts number in Col-0 (set at 1) for several independent T3 transgenic lines (*TER_{eri}*) obtained by complementation of *Coler105* (null mutant), *Coler2*, and Ler by Col-0 *ER* locus.

Copy number was quantified by real-time quantitative PCR. Data confirm complementation of all 3 mutants. *ERECTA* transcript abundance varied between transgenic lines but all lines displayed typical *ERECTA* morphological phenotypes, similar to those shown in Fig. 1C. Relative abundance was calculated after normalisation to copy number of 18S rRNA transcripts

Supplementary Figure 2



Phylogram of *ERECTA* and *ERECTA*-like genes based on analysis of sequence homology in the kinase domain (Gilmore et al., personal communication)

Analysis was done with PAUP using neighbour-joining and maximum parsimony methods, which examine similarity and evolutionary relatedness, respectively (support values in black or red, respectively; scale bar = 0.05 estimated amino acid substitutions per site).

ERECTA homologues were found in numerous species, whose sequences fall in two main groups of “ER” or “ERL” proteins, most closely related to AtER (At2g26330) or AtERL (At5g62230 and At5g07180), respectively. Those 2 groups (B and A) define putative *ERECTA* orthologues and paralogues, respectively, and appear to have evolved early in angiosperm evolution. At (*Arabidopsis thaliana*), Bo (*Brassica oleracea*), Eg (*Elaeis guineensis*), Gm (*Glycine max*), Hv (*Hordeum vulgare*), Le (*Lycopersicon esculentum*), Os (*Oryza sativa*), Sb (*Sorghum bicolor*), So (*Saccharum officinarum*), Ta (*Triticum aestivum*), Zm (*Zea mays*).

Supplementary Table 1. Characteristics of QTL TE1 in 4 different experiments using Composite Interval Mapping (QTL Cartographer software). R^2 denotes the proportion of total phenotypic variance explained by TE1; the additive effect describes the increase in Δ associated with the replacement of the *Columbia ERECTA* allele by the *Landsberg erl* allele.

Experiment/Growth conditions	LOD score at TE1	Additive effect (per mil)	R^2	Average Δ difference (per mil) associated with the presence of ColER vs Ler allele at ER marker
Growth chamber- 125 $\mu\text{E m}^{-2} \text{s}^{-1}$ 60% RH; 21°C 14h day-length	4.00	0.185	0.426	-0.365
Growth chamber- 490 $\mu\text{E m}^{-2} \text{s}^{-1}$ 50% RH; 21°C 10h day-length	8.07	0.231	0.533	-0.482
Glasshouse- 150-500 $\mu\text{E m}^{-2} \text{s}^{-1}$ 50% RH; 20/22°C 12h day-length	11.51	0.293	0.643	-0.436
Glasshouse- 200-700 $\mu\text{E m}^{-2} \text{s}^{-1}$ 65% RH; 20/25°C 12.5h day-length	3.57	0.211	0.209	-0.381

Supplementary Table 2. Difference in Δ between *erecta* mutants and several independent transgenic TER lines.

All values are expressed relative to Δ measured in Col-0. Complementation (lines denoted TER_{eri}) always led to significant decrease in Δ , hence increase in TE, compared to non-complemented transgenic lines (denoted Ter_i) or to the original mutants. Note that Δ in Col-1 (parental background of Coler2) and Col-4 (parental Columbia line N933 of RILs collection), were similar to each other and nearly the same as in Col-0 (data not shown).

GENOTYPE	LINE	$\Delta_{\text{LINE}} - \Delta_{\text{COL-0}}$ (PER MIL)
Coler2	N3140	+0.77
Ter2	143	+0.87
	154	+0.74
	247	+0.74
TER_{er2}	145	-0.16
	165	-0.20
	177	-0.42
	181	-0.28
	279	-0.35
	290	-0.30
Coler105		+1.22
Ter105	18	+1.55
	189	+1.39
TER_{er105}	29	+0.62
	46	+0.59
	55	+0.55
	61	+0.49
LdER	N163/3177	-0.23
Ler	NW20	+0.34
TER_{er1}	T3_7K	-0.49

ColER	Col-1(N3176)	-0.02
ColER	Col-4(N933)	+0.04

Supplementary data

Supplementary methods

Determination of carbon isotope composition and discrimination

Carbon isotope analyses were conducted with an Isochrom mass spectrometer (Micromass, Manchester, UK) coupled to a Carlo Erba elemental analyser (CE Instruments, Milan) operating in continuous flow mode. Carbon isotope ratios were obtained in δ -notation, where $\delta = R/R_{\text{standard}} - 1$ and R and R_{standard} are the isotope ratios of the plant sample and the VPDB standard, respectively. The $\delta^{13}\text{C}$ values were then converted to carbon isotopic discrimination values, $\Delta^{13}\text{C}$, using the equation: $\Delta^{13}\text{C} = (\delta_a - \delta_p)/(1 + \delta_p)$, where δ_a is the $\delta^{13}\text{C}$ of atmospheric CO_2 and δ_p is the $\delta^{13}\text{C}$ of the plant material. $\delta^{13}\text{C}$ of atmospheric CO_2 was assumed to be -8 per mil.

Relationship between Δ and TE

Transpiration efficiency, TE, is the ratio of CO_2 assimilation rate, A , to transpiration rate, E . Each of these fluxes is the product of a conductance to diffusion times a gradient in gaseous concentration. g is the conductance to diffusion of water vapour through the stomata. The conductance to CO_2 is 1.6 times less. The CO_2 partial pressure in the air is p_a and that in the intercellular spaces in p_i . The leaf-to-air vapour pressure difference is v . So, following⁶

$$TE = \frac{A}{E} = \frac{g(p_a - p_i)}{1.6g\nu} = \frac{p_a(1 - p_i/p_a)}{1.6\nu}$$

The discrimination, Δ , against CO_2 containing ^{13}C during photosynthesis is given by

$$\Delta = a + (b - a)p_i / p_a ,$$

where a is the fractionation during diffusion through the stomata ($\approx 4.4\%$, where $\%$ denotes per mil, or parts per thousand) and b is the effective fractionation by Rubisco [after taking into account diffusion from intercellular spaces to the sites of carboxylation] ($\approx 27\%$).

Combining these equations,

$$TE = \frac{p_a}{1.6v} \cdot \frac{b - \Delta}{b - a} .$$

Mutant complementation

pKUT196, a plasmid containing the entire *ERECTA* locus from *Columbia* was introduced into *Agrobacterium tumefaciens* strain AGL1 and used to transform *Coler2*, *Coler105* and *Ler* mutants by floral dipping. Selection of T1 transgenic plants was performed in Hoagland medium, on 0.75% agar plates containing $100 \mu\text{g ml}^{-1}$ gentamycin and $100 \mu\text{g ml}^{-1}$ timentin. All 46 gentamycin-resistant T1 plants displayed developmental and morphological phenotypes indistinguishable from the *Col-0* or *Landsberg N163* and *N3177* wild type plants (Fig. 1C and data not shown). Independent families were re-selected in the T2 and T3 generation on gentamycin plates to identify homozygous T3 lines.

Real-time quantitative PCR assays

Presence of the transgene and its expression in those lines was confirmed by real-time PCR. Total RNA was isolated with RNeasy Plant Kit (Qiagen, Hilden, Germany) from young rosettes, inflorescences and developing siliques of mutants and gentamycin

resistant T3 lines and digested with RNase-free DNaseI (product number D5307, Sigma-Aldrich, Taufkirchen, Germany). RT reactions were performed using QIAGEN OneStep RT-PCR kit according to the manufacturer's instructions in order to check efficiency of amplification and to generate standard dilutions series of products [*ERECTA* (*At2g26330* cDNA) and control normalizer 18S rRNA]. Amounts of *At2g26330* cDNA templates in samples were quantified by PCR reactions performed in a Rotorgene 2000 Thermal Cycler (Corbett Research, Sydney, Australia) using SYBR Green I to monitor product formation (final dilution of 1:40,000, Fisher Biotech, Springfield, NJ). Reactions contained 3 µl of QIAGEN OneStep RT-PCR Buffer 5x (containing 12.5mM MgCl₂), 2 µl RNase-free water, 0.6 µl 10mM dNTP mix, 0.6 µl QIAGEN OneStep RT-PCR Enzyme Mix, 0.3 µl 10X SYBR Green I, 1.5 µl 1U/µl RNasin Plus RNase Inhibitor (Promega), 1.5 µl of 5 µM primers, 25ng RNA or 5µl of serially diluted *ERECTA* cDNA and 18S rRNA standards (serial dilutions over at least 4 orders of magnitude). Primers used for the *ERECTA* cDNA were *At2g26330F* 5'-GTTAACCCGAAGGAAAGCCGTTGATG-3', and *At2g26330R* 5'-TCGGCTGTCTTTTGGTGCATAGGAGT-3', and for the 18s At18srRNA-F 5'-TCCGCCGGCACCTTATGAGAA-3', and At18srRNA-R 5'-GCGCGTGCGGCCAACA-3'. All reactions were carried out in triplicates. Data were analysed using Rotorgene software version 5.0.47 (Corbett Research, Sydney Australia), using the "two-standard curve method". *At2g26330* gene expression was normalised to that of 18S rRNA by subtracting the C_T value of 18S rRNA from that of *At2g26330*.